A trade-Off analysis between random noise attenuation and muscle state preservation: A simulation study on stretch reflex responses

Itai Heijmans

Abstract—The surface electromyographic (sEMG) signals that originate from skeletal muscle electrical activity, are used clinically and experimentally to determine muscular behaviour, e.g. amplitude, area under the curve and onset of activity. Surface EMG signals are inevitably contaminated by noise and artefacts from the site between the skin and electrodes, nontarget muscles and recording hardware. After recording, signal processing methods like filtering, are used in an attempt to determine the underlying active state of the muscle, portrayed by the motoneuron pool firing. As EMG is in fact a deformed representation of the actual muscle activity, processing is used to extract a more veracious description of the active muscle states. This study investigated the effects of random noise - which in practice resembles transducer noise -, and filtering on the simulation accuracy of short and long latency muscle stretch responses, extracted from simulated EMG signals. To obtain the deviation from the noiseless signals, a fiber potential model was developed to simulate the EMG surface potentials that used an existing motoneuron pool firing model by Schuurmans et al. 2009. The resulting EMGs were the muscle responses to stretch perturbations at different velocities and amplitudes combinations (1.5. 2, 3, 5 rad/s and 0.06, 0.10, 0.14 rad). Consecutively, the EMG signals were contaminated with different noise intensities (SNR: -1, 2, 5, 7, 9 dB) and then filtered with a 3rd order Butterworth lowpass filter, with cut-off frequencies between [1-200Hz]. Finally, the short- and long latency stretch responses areas were calculated and compared between the filtered noiseless and filtered noisy EMG signals, by calculating the difference between the values as a fraction of the value from the noiseless simulated signal. It was found that a signal-to-noise ratio of at least 5 dB with a 85Hz cut-off low-pass filter was necessary to keep the error below 10% maintaining M1 and M2 characteristics. It was also seen that M1 was more affected than M2 under the same amount of contamination, suggesting different spectral frequency contents between the stretch responses, and different underlying neuronal firing behaviour. The described signal-to-noise ratio thresholds and proposed cut-off frequencies resulting in acceptable signal error, can be used as a reference on accuracy of latency response simulations. The error courses provide information about the way error and signal are attenuated or preserved. Besides, the differences in error course comparing the two latency responses provides an insight into the difference in behaviour between the underlying reflex mechanisms. Apart from the findings the combination of adapted and developed model can be used in future research where noise-free surface potentials are required, and can be further developed to produce veracious EMG signals.

Index Terms-EMG, fiber potential modeling, Filtering, Noise

I. INTRODUCTION

Electromyography (EMG) is the recording and evaluation of the electrical action potentials generated from skeletal muscle fibers [1]. The potentials travel from the innervation zone,

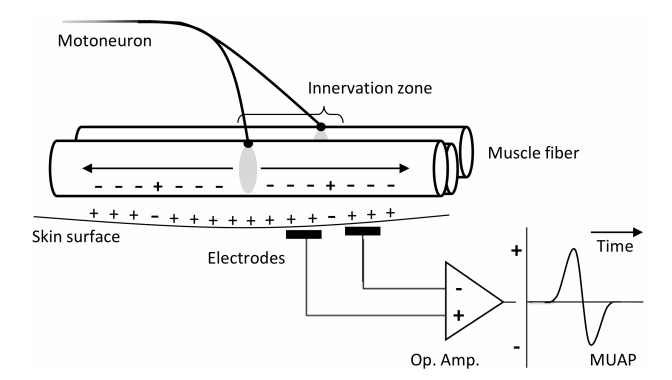


Figure 1: Schematic image of a motor unit action potential (MUAP) acquisition. The motoneuron axon innervates and activates a muscle fiber, creating an electrical potential, traveling along the fibre, creating an intracellular potential. The time-dependent contribution of the MUAP resembles a sinusoidal function, as the magnitude of the recorded potential is distance-dependent: The recorded MUAP intensity increases as the axial distance to the closest electrode decreases. At the minimal distance from the first electrode, a peak is reached, and when the distance is equal to either electrode, the summed potential cancels out and thus zero. Then, when the potential reaches the minimal distance to the second electrode, another (negative) peak arises creating a biphasic signal [5].

bi-directional with approximately 4m/s, along the fibers towards the tendons (see. Fig.1) [2]. The EMG is considered a super positioned sum of separate muscle fiber potentials originating from the active motor units, each potential having a specific amplitude and frequency. The propagating potentials can be estimated by their contribution with respect to the recording electrodes, then they are summed to the EMG signal by an operational amplifier [3]. Such a signal is called a motor unit action potential (MUAP), which amplitude and phase are mainly influenced by the depth of the recorded fibers inside the innervation zone and the distance between the recording electrodes, respectively.

EMG is often measured with electrodes on the skin covering the muscle of interest, this technique is called surface EMG (sEMG). sEMG is commonly used both clinically and experimentally, as it allows an easy and non-invasive measurement of muscle activity [2][4].

EMG signals can be difficult to interpret due to their stochastic nature [6], therefore signal processing is an important part of the acquisition. After recording, signal processing methods are operations that alter the acquired data in an attempt to

MSC THESIS: TU DELFT - OCTOBER 2019

determine the underlying active state of the muscle, portrayed by the motoneuron pool firing. As EMG is in fact a deformed representation of the actual muscle activity, processing is used to extract a more veracious description of the active muscle states. Typical EMG processing methods are rectification, smoothing and filtering. The latter also is frequently used to attenuate components of the recorded signal that are not considered part of the underlying muscle EMG signal, examples of which are; power line interference [7], motion artifacts [8] and cross talk from other muscles (e.g. ECG [9]) [10]. After filtering, the resultant EMG signals can be used as a measure of motoneuron pool activity. Commonly assessed EMG features are activation onset (see Fig.2) [11][12], peak amplitude [13] and magnitude of the short- (M1), and long latency responses (M2), which occur after an active muscle is stretched [14].

M1 is a response that follows after muscle stretch where muscle spindles are activated and induce afferent stimulation. This reflex is thus a result of activity of the monosynaptic circuit and predominantly velocity dependent. The long latency response is less well-understood and likely contains a compound response from multiple afferent inputs mediated by both spinal and supra-spinal pathways [15][16].

Getting a clear picture of EMG features is always a trade-off between the amount of noise-removal and muscle activity conservation. While the ultimate goal of using filters is to analyse noise-free signals, it is often unclear to what extent signal quality is really degraded by both noise and filtering methods. Research has shown how noise can change action potential shape and induce delays into onset simulations [17][18], filter use can also alter important signal properties which can skew their estimations [19]. An insight into the effects of filtering of contaminated signals on simulation of commonly assessed EMG features like stretch responses, could help future research appraise the accuracy of estimates.

This study investigated the effect of random noise on M1 and M2 area values, along with the trade-off between noise attenuation and degradation of electrical signals converted from binary motoneuron output. The random noise was chosen to mimic transducer noise [21]. The dynamics of this trade-

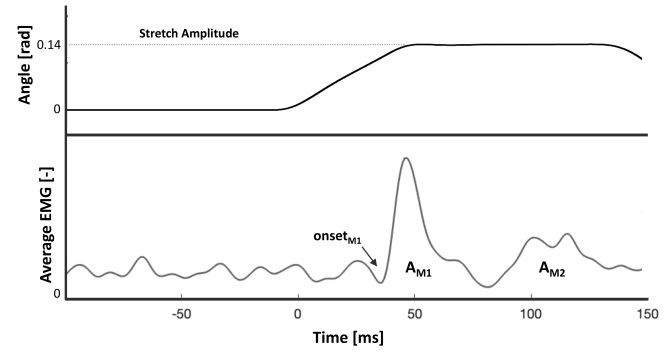


Figure 2: Top: Example of a ramp-and-hold perturbation of 0.14 radians, at a velocity of 3 rad/s eliciting a stretch reflex response. Bottom: The M1 and M2 areas and onset of the evoked reflex are indicated in a signal from the developed model.

off were related to the low-pass filter cut-off frequency. A muscle spindle model by Schuurmans et al. 2009, was used to obtain motoneuron output. The output was a neuronal firing response to stretch perturbations on a simulated muscle, with the properties of a flexor carpi radialis. Next, a model was built to simulate electrical activity (MUAPs) at muscle fiber level and convert this activity to skin surface potentials, from which noise-free and noisy EMG signals were created at different signal-to-noise ratio's. Lastly, after estimating the latency responses, the simulation error of the M1 and M2 responses areas were compared between noisy and noiseless signals for different low-pass filter cut-off frequencies.

2

II. METHODS

To evaluate the effect of noise on the simulations, noiseless and noisy EMG signals were generated. Ramp-and-hold perturbations with combinations of stretch amplitude and stretch velocity were simulated to elicit M1 and M2 responses on the flexor carpi radialis (see Fig.2).

Two models were combined to synthesize noise free EMG signals. First, a muscle spindle model from Schuurmans et al. 2009 [15] simulated the neuronal response to ramp-andhold stretch perturbations. Second, a fiber potential simulating model that produced an sEMG recording was built. The second model was fed with the output of the motoneuron pool model and produced 1.2 second signals. The functioning of the fiber potential model was checked by comparing a single MUAP shape and the M1 and M2-stretch velocity and amplitude relationship to findings in literature [22]. Consecutively, the simulated EMG signal was compared to the output of the spindle model and an experimentally recorded EMG (see Fig.4). Additionally, the motoneuron pool model and the fiber potential model outcomes were compared in terms of the M1/M2 response relationship for all stretch velocity and stretch amplitude combinations.

A. Models

1) Muscle spindle model

The muscle spindle model from Schuurmans et. al. 2009 [15] was used for this study. The model consisted of a motoneuron pool of 300 neurons innervated by tonic supra-spinal input for a constant torque, and a Ia afferent input from muscle spindles (see Fig.3). Each of the neurons in the pool received input from 100 tonic firing descending fibers and 120 Ia afferent fibers. The tonic input was 47 spikes per second to provide background activity of 10 spikes per second. The input from the muscle spindles as a response to stretch velocity and amplitude was given by a feline muscle spindle model that described bag_{1,2}- and chain fibers described by Mileusnic et al. [20]. The final output was the motoneuron pool's action potentials modeled as discrete events at every 1ms (i.e. 1 when a neuron fired, 0 when it did not). Twelve perturbation trials were simulated from the combinations of three stretch amplitudes (0.06, 0.10 and 0.14 rad) and 4 stretch velocities (1.5, 2, 3 and 5 rad/s). Each of the trials resulted in a 1.2 seconds signal with a 1000Hz resolution.

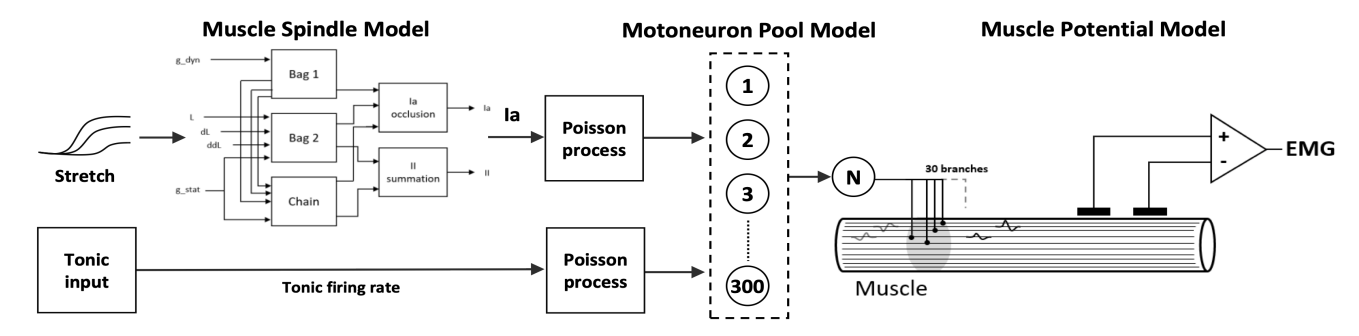


Figure 3: Schematic representation of the process converting stretch and tonic input, to recorded EMG output with the used models. (left to right): Simulink muscle spindle model by Mileusnic [20] to produce Ia and tonic firing as a result of ramp-and-hold stretch perturbations. Motoneuron pool model integrated with the muscle spindle model by Schuurmans et al. 2009. The MUAP simulating model converting the motoneuron firing into EMG signal by simulation of the neuron-to-fiber branching, potential travel and recorded potential contribution resulting in an EMG signal.

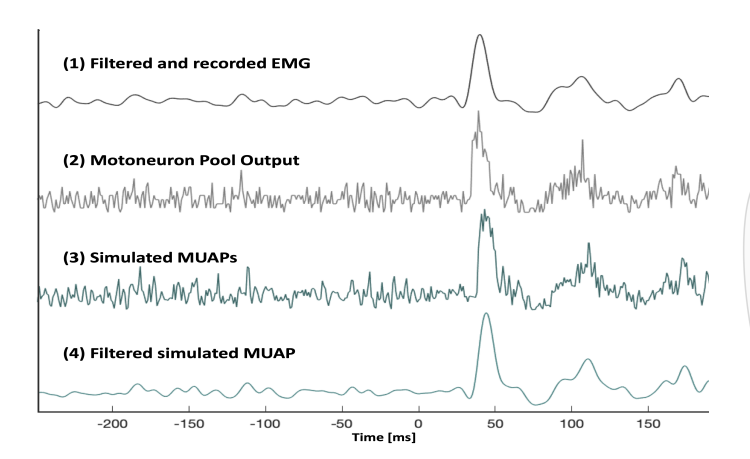


Figure 4: Experimentally recorded (1) and simulated (2,3 and 4) signals from a perturbation with stretch amplitude 0.14 rad and velocity 2 rad/s. Top to bottom: Recorded signal by Schuurmans et al. 2009, Motoneuron pool output Schuurmans et al. 2009, MUAP simulating model output, filtered MUAP simulating model output. All signals were 3rd order low-pass Butterworth filtered, at 80Hz cut-off). Additional comparisons can be found in Fig.8.

2) Fiber potential model

To transform motoneuron pool's action potentials into an EMG signal, a model was required to translate the binary input from the muscle spindle model into electrical activity at muscle fiber level. First, the flexor carpi was modelled as a cylinder with a length of 158.5mm and a radius 12.4mm, equal to the muscle dimensions described by Schuurmans et. al. 2009 [15]. The muscle's motor units were realized by randomly assigning 30 muscle fibers to each of the 300 motoneurons, resulting in a density of ~ 15 fibers/mm² [23]. Innervation points and therefore muscle fiber locations, could not overlap in the YZ-plane (see Fig.5). The innervation zone was created by randomly scattering 9000 points (300 neurons×30 fibers) in a cylindrical ring within the modeled muscle with a radius of 12.4mm and a length of 5mm [24], [25]. The motoneurons were programmed to activate fast muscle fibers in the outer region of the muscle, considering the type of contraction (reflex) [26]. Above mentioned arrangement emulated the branching of axons onto a group of nearby muscle fibers. Hence, adjacent muscle fibers did not necessarily belong to the same motor

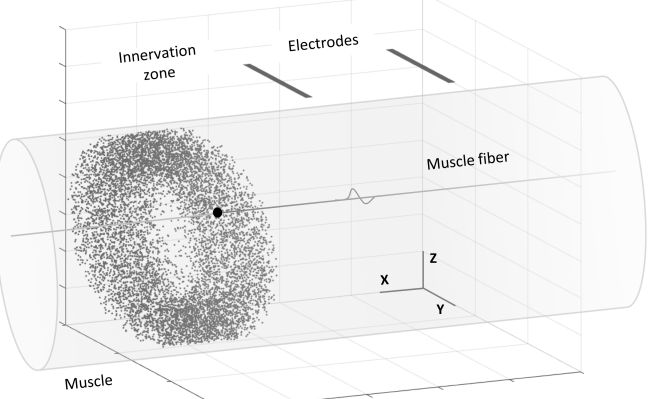


Figure 5: 3-Dimensional representation of the simulated innervation zone inside the muscle and electrodes on its surface. The innervation zone shows the 9000 points where individual muscle fibers are innervated. One muscle fiber is shown, the black dot indicates the location where the fiber is innervated. For illustrative purpose a propagating potential in one direction is shown.

unit and each individual muscle fiber was innervated by only one neuron [27]. Fiber thickness was assigned from a Gaussian distribution with a mean of $55\mu m$ diameter and a standard deviation of $9\mu m$ [27]. The muscle fiber conduction velocity (MFCV - pulse propagation along the fiber length), was dependent on the muscle fiber thickness (MFD, 'd'), according to the relationship: MFCV=0.05×MFD+0.95 [28]. Finally, two recording bar-shaped electrodes (Delsys Bagnoli, contact dimensions: 10x1mm) were simulated 5mm above the most superior muscle fiber with a 10mm spacing between each other along the muscle fiber length.

3) MUAP generation

To produce an EMG signal, the potential contribution of each activated muscle fiber to a point on the electrode was calculated at every time step, while the current travels from the innervation zone, bi-directionally, towards the tendons. The muscle was considered to be cylindrically anisotropic in terms of its conducting properties [29]. The method to calculate the potential contribution was adapted from Nandedkar et al. 1985 [30]. The potential contribution can be obtained by convoluting the transmembrane current contribution i(t) with a weight

function w(t) [22], [30], [31]:

$$AP_n(t) = i(t) * w(t) = F^{-1}[I(\omega)W(\omega)]$$
 (1)

$$I(\omega) = F[i(t)], W(\omega) = F[w(t)]$$
 (2)

Where F denotes a Fourier transform. As described by Rosenfalck et al. 1969[32], the transmembrane current is proportional to the second derivative of the intracellular potential. The current can be summed over the fiber axis, expressed as:

$$i_m(x) = \frac{\sigma_i \pi d^2}{4} p_i''(x) \tag{3}$$

d: muscle fiber diameter

 σ_i : intracellular conductivity (1.01 S)

 $p_i(x)$: intracellular potential

in previous work[31], the intracellular potential was expressed as

$$p_i(x) = 768x^3e^{-2x} - 90 (4)$$

Therefore, the second derivative of $p_i(x)$ was

$$p_i''(x) = 1536e^{-2x}(3x - 6x^2 + 2x^3)$$
 (5)

As stated by Nandedkar 1983, the electrical potential Φ , of the current source in the muscle fiber's coordinate system's origin at point (r,x) is defined as follows:

$$\Phi(r,x) = \frac{I}{4\pi\sigma_r\sqrt{Kr^2 + x^2}}\tag{6}$$

Where,

I: strength of the current source (388 μ A)

K: σ_x/σ_r

 σ_x : axial conductivity (0.33 S/m)

 σ_r : radial conductivity (0.063 S/m)

With r and x being the radial and axial distance, respectively in the YZ-plane.

The simulated recording electrodes had a rectangular contact area, where thus far the contributions were considered with respect to a point-shaped electrode. Therefore, the contributions with respect to the electrode surface were calculated using the weight function. The weight function is determined by integrating $\Phi(r,x)$ over the surface of the electrode. Considering the location of the unit source at coordinates $[x_0,y_0,z_0]$, and $[x,y_{el.1},z]$ to $[x,y_{el.2},z]$ for the electrode along the y-axis, the recorded potential by the first electrode is

$$\frac{1}{4\pi\sqrt{K}}\ln\left[\frac{y_2 - y_0 + \sqrt{(y_2 - y_0)^2 + B}}{y_1 - y_0 + \sqrt{(y_1 - y_0)^2 + B}}\right] \tag{7}$$

For $y_{el.1} < y_0 < y_{el.2}$

$$\frac{1}{4\pi\sqrt{K}}\ln\left[\frac{y_1-y_0+\sqrt{(y_1-y_0)^2+B}}{y_2-y_0+\sqrt{(y_2-y_0)^2+B}}\right]$$
(8)

For $y_{el,2} < y_0 < y_{el,1}$ where

B:
$$(y-y_0)^2 + (z-z_0)^2/K$$

Finally, taking the inverse Fourier transform of the product of the Fourier transform of both the current contribution and the weight function, the potential contribution is calculated (see Eq.2).

4

As previously mentioned, the sample frequency used for the developed fiber potential model as well as the muscle spindle model was 1000Hz. Hence, each 1 ms the voltage output of the pulses propagating along activated muscle fibers was summed for both recording electrodes. The MUAP shape behaviour was tested as a response to distance-to-electrode and electrode spacing where amplitude decreased with increasing distance-to-electrode and phase increase with electrode spacing, as expected.

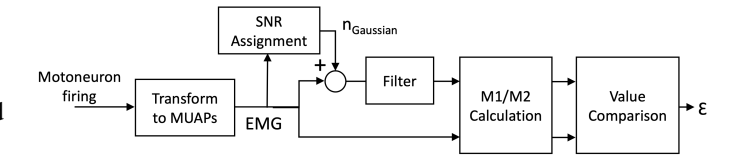


Figure 6: Schematic representation of the processing approach from motoneuron firing to error calculation. $n_{Gaussian}$: White Gaussian noise, ϵ : error between simulated noiseless M1/M2 value and the same value skewed by noise per cut-off frequency setting.

B. Procedures

1) Filter settings and noise

To find the effect of the noise on the stretch reflex responses simulations, two types of signals were prepared for the trials; (1) the simulated EMG, (2) simulated EMG + white noise. The random noise was chosen to mimic transducer noise, which is caused by differences in the impedance between the skin and the electrode, and from redox reactions occurring in the contact region between the electrode and the conductive gel [21].

Five noise intensities were included into the trials: SNR - 1, 2, 5, 7 and 9dB, for their prevalence in literature and experimental cases [18], [33]. Therefore, the 12 combinations of velocity and amplitude were each contaminated with the five noise levels. Adding the random noise to the EMG signals was achieved using the MATLAB function *awgn*, which computes a ratio of the input signal's summed squared magnitude to that of the noise [34]. Next, the noisy signals were rectified and then filtered with a 3rd order Butterworth low-pass filter with cut-off frequencies from 1-200Hz, with a 1Hz step size. The signals were filtered using MATLAB's *filtfilt* function to minimize phase shift, the processing methods are presented schematically in Fig.6.

2) Stretch reflex responses

For the noiseless and noisy EMG signals, the short and long latency responses were determined. The M1 response considered between 20 and 50 ms after stretch onset and the M2 response between 55 and 100 ms after stretch onset [35]. Each signal was normalized with respect to the mean background activity, then the area under the curve for M1 and M2 were calculated. To ensure reproducible results from both the motoneuron pool model as well as the fiber potential model

MSC THESIS: TU DELFT - OCTOBER 2019

the randomization algorithm was reset throughout the program (MATLAB function rng('default')).

3) Stretch reflex simulation error

To quantify the effect of filtering on the accuracy of stretch reflex responses, the errors (ϵ) from the noisy signals were computed: The M1 and M2 values for all combinations of stretch velocities and amplitudes were calculated for both the unfiltered noiseless and filtered contaminated signals and then subtracted from the M1 and M2 of the noiseless unfiltered signals, finally they were divided by the noiseless unfiltered values to represent the error relative to the 'true' value (see Eq.9).

$$\epsilon_{M1} = \left| \frac{M1_{simulated} - M1_{contaminated}}{M1_{simulated}} \right| \tag{9}$$

To verify that the noiseless signal would change most where filter order was highest and cut-off frequency lowest, a test was done comparing the difference brought upon the signal as a function of the two filter settings. This was tested in order to verify the expectation behind the noise and EMG filtering relation; (decreasing cut-off attenuates both EMG and noise signal). The outcome is shown in Fig.7, which shows the cumulative difference for varying the three filter orders and cut-off frequencies, for all four stretch velocities and two stretch amplitudes, 0.06 and 0.14 rad.

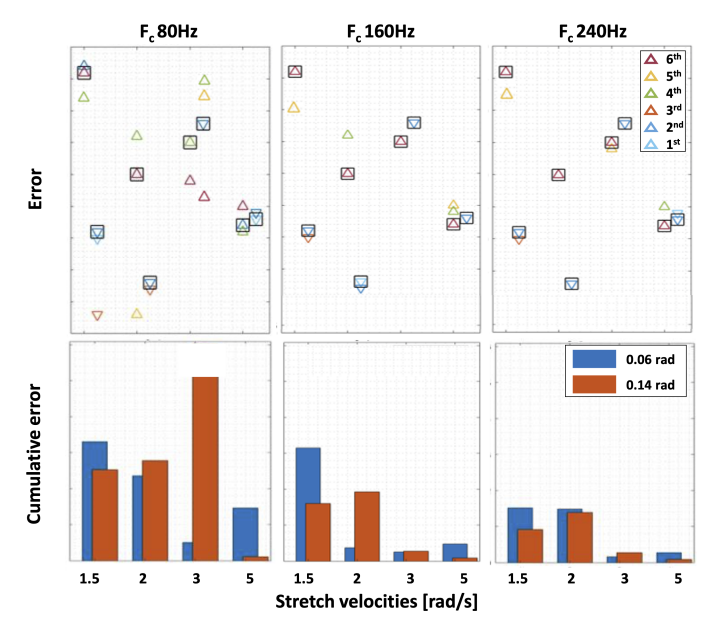
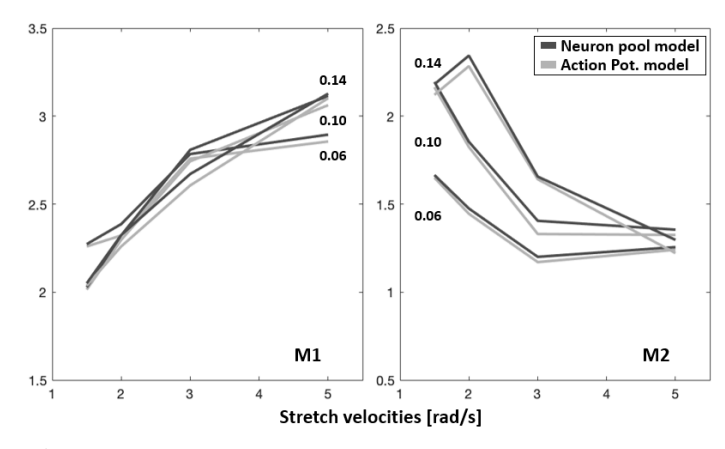


Figure 7: Visualization of the effect of the filter cut-off frequency and order on the error between filtered and unfiltered noiseless EMG for the M1 area. column 1st column: cut-off frequency 80Hz. 2nd column: cut-off frequency 160Hz. 3rd column: cut-off frequency 240Hz. Increasing cut-off frequency while decreasing the difference from pure EMG. Row 1: scatter plots per cut-off frequency showing filtered data points in colored triangles and simulated EMG data points in black boxes, row 2: the summed deviation between unfiltered noiseless data and filtered noiseless data, per stretch velocity. (box locations depend on stretch velocity and amplitude combination, model order indicated by color) \triangle : 0.06 rad filtered ∇ : 0.14 rad filtered \square : unfiltered simulated EMG M1 area value.



5

Figure 8: Plots of M1 and M2 magnitude (stretch amplitude and velocity) relation produced by the motoneuron pool model Schuurmans 2009, and the fiber potential model. The stretch amplitudes 0.06, 0.10 and 0.14 rad, are indicated per line. Mean error between models was 0.014 for M1 and 0.016 for M2: calculated as the mean difference between values of each amplitude-velocity combination, for both models and expressed as a fraction of neuron pool model values.

III. RESULTS

A. Model comparisons

The average error between M1 plots and M2 plots, comparing the motoneuron pool model and the fiber potential model suggests that using neuron pool firing is nearly equivalent to using the sEMG signal that the motoneuron pool firing results in (see Fig.8). Therefore, the velocity-amplitude-reflex response relationships found in [15] still hold.

In Fig.9 the effect of noise at three intensities and filtering is visualised. A signal from a perturbation of 2 radians at 3 radians/s, was contaminated with three levels of noise. All three signals were filtered with a 3rd order Butterworth filter, cut-off at 80Hz. Additionally, an experimentally recorded and filtered signal by Schuurmans 2009. is shown for the same amplitude-velocity perturbation combination. It is seen that higher SNR shows more variation in both the unfiltered and filtered signals. The signal with the highest SNR resembles the recorded and filtered EMG signal most. The noise contribution throughout the signal influences the M1 and M2 both in shape and size.

B. M1 and M2 stretch velocity-amplitude relation

The results of the shape and size change of M1 and M2 are displayed in Fig.10, where noisy and noiseless (SNR= ∞) signals were used to plot M1 and M2 velocity-amplitude relations, using the same filter setting as Fig.9. The influence of the amount of noise is shown for M1 and M2 from the simulated unfiltered and filtered signals. Especially comparing the extremes (SNR: -1dB and 7dB), the plots show how the relation between stretch velocity and stretch amplitude in terms of magnitude of the responses is altered; for M1 resulting from noiseless EMG signals, a linear relationship between stretch velocity and magnitude exists, stretch amplitude has no influence as all three stretch amplitude

MSC THESIS: TU DELFT - OCTOBER 2019

- 6

lines deviate little along the Y-axis. However, considering the relationship for the three SNR levels, it can be seen how the amount of noise presence influences this relationship. The same linear relationship between velocity and magnitude of M1 is less distinguishable and a normally non-existent effect of stretch amplitude is seen, as the difference in M1 magnitude increases.

Considering the M2 plots, the negative linear relationship still holds, although the shape of the plots is compromised: the size of the error between the stretch amplitude plots appears to decrease with higher stretch velocity. Additionally, both in M1 and M2 plots, the errors for 0.10 rad perturbation are consistently largest.

1) Cut-off frequency and error relation

The errors of M1 and M2 observed in Fig.10, were further investigated along with the effect of cut-off frequency on the course of the error. The error between M1 and M2 values that were contaminated by one of five noise intensities, and the simulated noiseless EMG signals is shown as a function cut-off frequency range 1-200Hz, for a 3rd order Butterworth low-pass filter in Fig.11. For both M1 and M2, the error decreases as the cut-off frequency increases. The error in M1 declines to zero for a lower cut-off frequency than M2. As the noise presence was equal for all combinations of stretch amplitude and velocity, suggesting a difference in frequency content. Between 7 and 9dB little difference is seen, suggesting that increasing the SNR above 7dB does not contribute in the same amount as increasing the SNR by 2dB in the -1 to 7dB range.

Considering the 5dB SNR, which is a realistic signal to noise ratio in EMG recordings [18], in case of M1, the error does not further decrease below 10% consistently after 75 Hz, which suggests a point where a balance is encountered between noise attenuation and signal preservation. In case of the M2, however, the 5 dB SNR course resembles the 7 and 9 dB courses much more as all lie close together, but after 85 Hz does not decline below 5% error consistently. Meaning that the balance between noise attenuation and signal preservation is reached at a higher cut-off frequency and ultimately reaches a smaller error than when M1 is estimated.

Lastly, considering the lowest SNR (-1dB) for M1 simulation, Fig.11 shows that the error does not decrease below 23%, making signals with such SNR unsuitable for M1 area measurement. For M2 Fig.11 shows how the error is much lower across the frequency range, compared to M1, as it lies between 10-20%. The variability of the course of the error however is high, as the error can change up to 7% over the course of only 8Hz (seen between 80-100Hz). Comparing the changes on M1 and M2 magnitude introduced by the noise, M1 is clearly more affected than M2. The difference of impact is seen when considering the dispersion of the plot-lines for both the short and long latency response. These error courses over cut-off

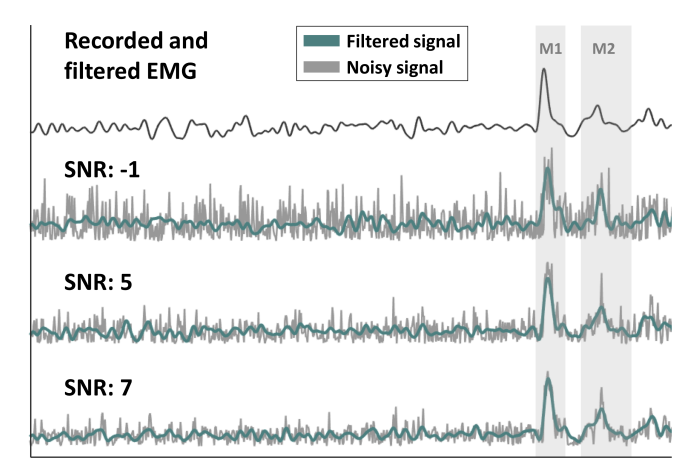


Figure 9: Visualisation of the effect of noise and filtering on EMG signals contaminated with white Gaussian noise for three SNR levels. The top signal, is an experimentally recorded and filtered signal by Schuurmans et al. [15], the 2nd 3rd and 4th signals are simulated by the fiber potential model. All signals are Butterworth 3rd order low-pass filtered at 80Hz cut-off and elicited by perturbations at 0.14 rad, 5 rad/s.

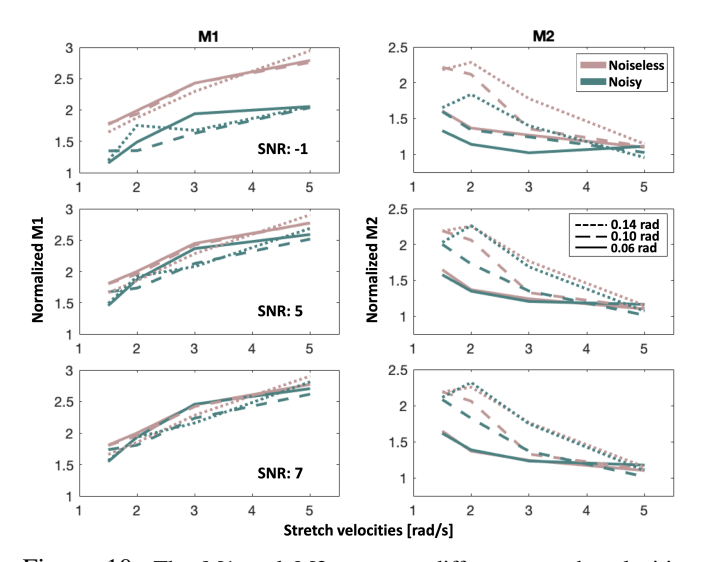


Figure 10: The M1 and M2 areas at different stretch velocities and amplitudes for noisy and noiseless EMG signals. SNRs (top to bottom): -1, 5 and 7 dB. Stretch amplitude line styles [rad]: 0.06 line, 0.10 dashed, 0.14 dotted.

frequency show that for M1 and M2 simulation, for signals with SNR 5dB, an error of under 10% can be achieved by using a cut-off frequency of 80Hz. An interesting finding seen in Fig.11, was that when comparing the error course for the low cut-off frequencies (0-27Hz), M2 showed highest errors for signals with the lowest noise presence. Compared to the same range for M1, errors were highest for the lowest SNR, as expected and as is visible over the entire cut-off frequency range, both for M1 and M2.

MSC THESIS: TU DELFT - OCTOBER 2019 7

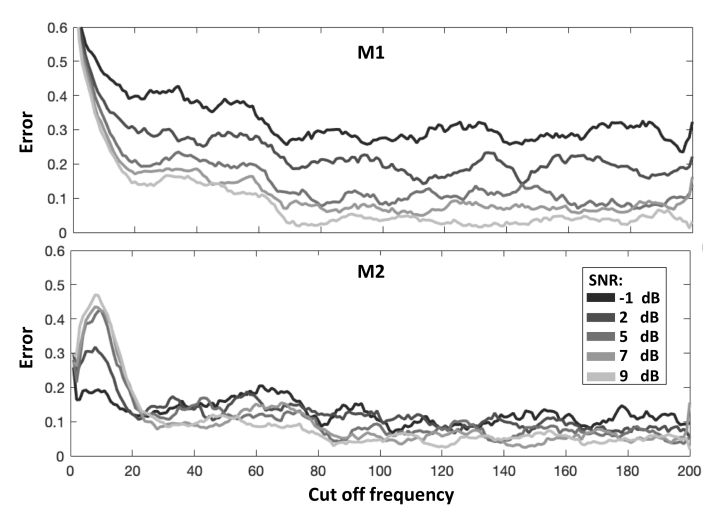


Figure 11: (top M1, bottom M2). The error courses displayed are relative to unfiltered simulated noiseless EMG value and is displayed as function of cut-off frequency for five signal-to-noise ratio's. The error is averaged over all combinations of stretch velocity-amplitude combinations. Filter used: low-pass Butterworth 3rd order.

IV. DISCUSSION

The present study investigated the effect of noise contamination on the simulation of the short latency and long latency stretch response, along with the trade-off between noise attenuation and signal degradation by low-pass filtering. A model was developed to convert binary neuron firing signals from an existing model, into simulated surface potentials to form EMG signals. The obtained signals were contaminated with white Gaussian noise and low-pass filtered for a range of cut-off frequencies (range?). Next the areas of short latency and long latency reflexes (M1 and M2) were calculated as a function of stretch velocity, for three stretch amplitudes. The area calculations were done for both the noiseless and contaminated signals. Finally, errors were calculated between M1 and M2 values extracted from contaminated signals and the ones from noiseless EMG signals.

A. Error size effect and cut-off recommendation

The study revealed that short-, and long-latency response simulations could be heavily altered by random noise contamination, skewing existing stretch velocity and amplitude relationships. Errors $\leq 10\%$ maintained the amplitude-velocity relationships as found by Schuurmans et al 2009. For signals with SNRs lower than 5dB, the $3^{\rm rd}$ order low-pass filter could not decrease errors consistently to under 10% within the 1-200Hz cut-off frequency range, neither for M1 nor M2.

For SNRs of 5dB and higher, a cut-off frequency of at least 80Hz (for M1) and 85Hz (for M2) was necessary to maintain validity of stretch amplitude and stretch velocity relationships of the latency responses, and keep the average error below 10%. It was also concluded that simulation accuracy of the short latency response was worse by equal amounts of noise at equal filtering methods, compared to the long latency response. As shown in Fig.11, M1 error is visibly higher than M2, for the same cut-off, and as noise contributions are equal, this

indicates a higher magnitude and/or frequency presence in the 20-65Hz region.

Part of the results featured a contradicting finding that could not readily be explained: where overall the lowest errors were seen for the highest signal-to-noise ratio's, in case of the error course of M2, the opposite was found in the lowest cut-off frequency range (0-25Hz). As added noise was completely equal for every signal contamination, it is very unlikely that the difference can be attributed to the noise contribution. Therefore, a difference in frequency contents between M1 and M2 could explain the discrepancy. The error course between 0-25Hz, might be explained by a high presence of frequencies in this region for M2, where with high SNR, using low cut-off frequency, significant portions of the spectrum are attenuated. This is translated to the contributions in time domain, which are used for the area calculations, resulting in a high error. As SNR decreases, more noise is attenuated or coincidentally contributed to a recovery of M2 features in this frequency range.

B. Limitations and recommendations for future research

An important basis on which the conclusions were drawn in this work, was the type of noise used to contaminate the EMG signals. The random noise used here, does not represent completely the contamination EMG signals can be corrupted by in experimental settings. Namely, recording EMG often means recording power line interference, motion artifacts and when recording trunk muscles, ECG noise. Findings in this work could therefore be strengthened, would they be conducted under conditions where added noise resembled experimentally recorded signal corruptions better.

The other important factor leading to the findings was the generated EMG signal. As mentioned before, mimicking experimental conditions helps improve the validity of the outcomes and several factors such as muscle and muscle fiber shape, quantity and composition, non-ideal electrode positioning could improve their factuality, as these influence the motor unit action potential.

In previous work that simulated EMG, higher quantities (~40000) of muscle fibers were simulated for smaller muscles than the flexor carpi radialis in this work, for which 9000 fibers were simulated [36]. As pulses from motoneurons were pseudo-randomly assigned to muscle fibers, smaller muscle fiber pools can introduce bias, where certain regions of the modeled muscle are excited significantly more than others. Therefore, a bias towards exciting regions closer or further away from the recording sites could exist. Electrode distance has been shown to influence the MUAP's amplitude and mean power frequency, also, muscle fibers within the proximity of 10-12mm from the electrode have been shown to dominate the contribution to the signal energy [37]. Therefore, a bias towards activation of certain regions can influence factors determining the M1 and M2 area.

Other filtering settings than cut-off frequency were not taken into account in this study. Different types of filters than

REFERENCES

the Butterworth filter, and other orders than 3rd could have different outcomes than the ones in the present work. Also, the effect of the used filter has been limited to the area of the short and long latency responses, where onset detection or/and peak detection could be influenced by the filtering method differently. Additional research is therefore needed, simulating recorded EMG as truthful as possible, using a larger variety of methods to help create a more complete picture of the best ways to prepare EMG signals before analysis.

The described signal-to-noise ratio thresholds and proposed cut-off frequencies resulting in acceptable signal error, can be used as a reference or prior knowledge on the simulation accuracy of latency response simulations. The error courses provides information about the way error and signal are attenuated or preserved. Besides, the differences in error course comparing the two latency responses provides an insight into the difference in behaviour between the underlying mechanisms. The combination of adapted and developed model can be further refined and used to accurately estimate surface EMG signals and the dynamics thereof.

C. Conclusions

- The study revealed adverse effects of random noise in EMG signals, on accuracy of latency response calculations.
- With the help of the Butterworth low-pass filtering, insight to the underlying muscle activity state of contaminated stretch reflex responses can be improved.
- There is little difference between using motoneuron pool firing and MUAP potentials in short, and long latency magnitude simulations (Fig.8).
- Random noise contamination below 5dB SNR, can skew stretch amplitude-velocity relations up to 30%.
- To maintain stretch amplitude-velocity relations for both short, and long latency responses, EMG signals with SNRs > 5dB need to be low-pass filtered with at least a 3rd order filter at 85Hz cut-off frequency.
- Short- and long latency responses are not to the same extent affected by random noise contamination, seen from their non-similar error courses, which suggests a difference in frequency contents.

REFERENCES

- [1] T. M. Dictionary. (2019). Electromyography, definition of, [Online]. Available: https://medical-dictionary.thefreedictionary.com/electromyography (visited on 09/03/2019).
- [2] R. Merletti, P. A. Parker, and P. J. Parker, *Electromyography: physiology, engineering, and non-invasive applications*. John Wiley & Sons, 2004, vol. 11.
- [3] A. S. Blum and S. B. Rutkove, *The clinical neurophysiology primer*. Springer, 2007, vol. 388.
- [4] M. Yunfen Wu Maria Angeles and P. O. Balaguer, Overview of the Application of EMG Recording in the Diagnosis and Approach of Neurological Disorders. Intech Open Science, 2013, vol. 1.

[5] K. Nishihara, Y. Chiba, Y. Suzuki, H. Moriyama, N. Kanemura, T. Ito, K. Takayanagi, and T. Gomi, "Effect of position of electrodes relative to the innervation zone onsurface emg", *Journal of medical engineering & technology*, vol. 34, no. 2, pp. 141–147, 2010.

- [6] N. Nazmi, M. Abdul Rahman, S.-I. Yamamoto, S. Ahmad, H. Zamzuri, and S. Mazlan, "A review of classification techniques of emg signals during isotonic and isometric contractions", *Sensors*, vol. 16, no. 8, p. 1304, 2016.
- [7] M. Malboubi, F. Razzazi, and S. M. Aliyari, "Elimination of power line noise from emg signals using an efficient adaptive laguerre filter", in *ICSES 2010 International Conference on Signals and Electronic Circuits*, IEEE, 2010, pp. 49–52.
- [8] Y. Hu, X. Li, X. Xie, L. Pang, Y. Cao, and K. Luk, "Applying independent component analysis on ecg cancellation technique for the surface recording of trunk electromyography", in 2005 IEEE Engineering in Medicine and Biology 27th Annual Conference, IEEE, 2006, pp. 3647–3649.
- [9] C. J. De Luca, L. D. Gilmore, M. Kuznetsov, and S. H. Roy, "Filtering the surface emg signal: Movement artifact and baseline noise contamination", *Journal of biomechanics*, vol. 43, no. 8, pp. 1573–1579, 2010.
- [10] M. Reaz, M. Hussain, and F. Mohd-Yasin, "Techniques of emg signal analysis: Detection, processing, classification and applications (correction)", *Biological procedures online*, vol. 8, no. 1, pp. 163–163, 2006.
- [11] F. Lacquaniti and J. Soechting, "Emg responses to load perturbations of the upper limb: Effect of dynamic coupling between shoulder and elbow motion", *Experimental Brain Research*, vol. 61, no. 3, pp. 482–496, 1986
- [12] C. Gielen, L. Ramaekers, and E. Van Zuylen, "Long-latency stretch reflexes as co-ordinated functional responses in man.", *The Journal of physiology*, vol. 407, no. 1, pp. 275–292, 1988.
- [13] G. Loudon, N. Jones, and A. Sehmi, "New signal processing techniques for the decomposition of emg signals", *Medical and Biological Engineering and Computing*, vol. 30, no. 6, pp. 591–599, 1992.
- [14] J. C. Rothwell, P. D. Thompson, B. L. Day, J. Dick, T. Kachi, J. Cowan, and C. D. Marsden, "Motor cortex stimulation in intact man: 1. general characteristics of emg responses in different muscles", *Brain*, vol. 110, no. 5, pp. 1173–1190, 1987.
- [15] J. Schuurmans, E. de Vlugt, A. C. Schouten, C. G. Meskers, J. H. de Groot, and F. C. van der Helm, "The monosynaptic ia afferent pathway can largely explain the stretch duration effect of the long latency m2 response", *Experimental brain research*, vol. 193, no. 4, pp. 491–500, 2009.
- [16] I. M. Tarkka, "Short and long latency reflexes in human muscles following electrical and mechanical stimulation.", *Acta physiologica Scandinavica. Supplementum*, vol. 557, pp. 1–32, 1986.

- [17] Y. St-Amant, D. Rancourt, and E. A. Clancy, "Effect of smoothing window length on rms emg amplitude estimates", in *Proceedings of the IEEE 22nd Annual Northeast Bioengineering Conference*, IEEE, 1996, pp. 93–94.
- [18] G. Allison, "Trunk muscle onset detection technique for emg signals with ecg artefact", *Journal of Electromyography and Kinesiology*, vol. 13, no. 3, pp. 209–216, 2003.
- [19] D. Stashuk, "Emg signal decomposition: How can it be accomplished and used?", *Journal of Electromyography and Kinesiology*, vol. 11, no. 3, pp. 151–173, 2001.
- [20] M. P. Mileusnic, I. E. Brown, N. Lan, and G. E. Loeb, "Mathematical models of proprioceptors. i. control and transduction in the muscle spindle", *Journal of neurophysiology*, vol. 96, no. 4, pp. 1772–1788, 2006.
- [21] B. Gerdle, S. Karlsson, S. Day, and M. Djupsjöbacka, "Acquisition, processing and analysis of the surface electromyogram", in *Modern techniques in neuro*science research, Springer, 1999, pp. 705–755.
- [22] S. Nandedkar, E. St, *et al.*, "Simulation of single muscle fibre action potentials", *Medical and Biological Engineering and Computing*, vol. 21, no. 2, pp. 158–165, 1983.
- [23] T. U. of Texas McGovern Medical School. (2006). Neuroscience: Motor units and muscle receptors ch1, [Online]. Available: https://nba.uth.tmc.edu/neuroscience/m/s3/chapter01.html (visited on 08/11/2019).
- [24] D. Pette and R. S. Staron, "Mammalian skeletal muscle fiber type transitions", in *International review of cytology*, vol. 170, Elsevier, 1997, pp. 143–223.
- [25] K. Saitou, T. Masuda, D. Michikami, R. Kojima, and M. Okada, "Innervation zones of the upper and lower limb muscles estimated by using multichannel surface emg", *Journal of human ergology*, vol. 29, no. 1-2, pp. 35–52, 2000.
- [26] R. Dahmane, S. Djordjevič, B. Šimunič, and V. Valenčič, "Spatial fiber type distribution in normal human muscle: Histochemical and tensiomyographical evaluation", *Journal of biomechanics*, vol. 38, no. 12, pp. 2451–2459, 2005.
- [27] A. Hamilton-Wright and D. W. Stashuk, "Physiologically based simulation of clinical emg signals", *IEEE Transactions on biomedical engineering*, vol. 52, no. 2, pp. 171–183, 2005.
- [28] P. J. Blijham, H. J. Ter Laak, H. J. Schelhaas, B. Van Engelen, D. F. Stegeman, and M. J. Zwarts, "Relation between muscle fiber conduction velocity and fiber size in neuromuscular disorders", *Journal of Applied Physiology*, vol. 100, no. 6, pp. 1837–1841, 2006.
- [29] P. Malmivuo, J. Malmivuo, and R. Plonsey, *Bioelectromagnetism: principles and applications of bioelectric and biomagnetic fields*. Oxford University Press, USA, 1995.
- [30] S. Nandedkar and E. Stålberg, "Simulation of macro emg motor unit potentials", *Electroencephalography and clinical Neurophysiology*, vol. 56, no. 1, pp. 52–62, 1983.

- [31] S. D. Nandedkar, E. V. Stalberg, and D. B. Sanders, "Simulation techniques in electromyography", *IEEE Transactions on biomedical engineering*, no. 10, pp. 775–785, 1985.
- [32] P. Rosenfalck, "Intra-and extracellular potential fields of active nerve and muscle fibres", *Acta Phisiologica Scandinavica*, vol. 321, 1969.
- [33] G. Lu, J.-S. Brittain, P. Holland, J. Yianni, A. L. Green, J. F. Stein, T. Z. Aziz, and S. Wang, "Removing ecg noise from surface emg signals using adaptive filtering", *Neuroscience letters*, vol. 462, no. 1, pp. 14–19, 2009.
- [34] signal-to-noise-ratio matlab, https://nl.mathworks.com/ help/signal/ref/snr.html, Accessed: 2019-10-08.
- [35] G. N. Lewis, E. J. Perreault, and C. D. MacKinnon, "The influence of perturbation duration and velocity on the long-latency response to stretch in the biceps muscle", *Experimental brain research*, vol. 163, no. 3, pp. 361–369, 2005.
- [36] W. Yao, R. J. Fuglevand, and R. M. Enoka, "Motor-unit synchronization increases emg amplitude and decreases force steadiness of simulated contractions", *Journal of Neurophysiology*, vol. 83, no. 1, pp. 441–452, 2000.
- [37] A. J. Fuglevand, D. A. Winter, A. E. Patla, and D. Stashuk, "Detection of motor unit action potentials with surface electrodes: Influence of electrode size and spacing", *Biological cybernetics*, vol. 67, no. 2, pp. 143–153, 1992.